Molecular and Electronic Structures of Model Compounds of Doped Polyacetylene

Chizuko TANAKA and Jiro TANAKA*
Department of Chemistry, Faculty of Science, Nagoya University, Chikusa, Nagoya, 464-01
(Received July 9, 1992)

Using the ab initio HF SCF MO method optimized molecular structures were calculated on twenty five model compounds of doped polyacetylene, which were charge-transfer complexes between dopants (Na, Li, and Cl atoms) and *trans*-polyenes (C_6H_8, C_8H_{10}, $C_{12}H_{14}$, $C_{14}H_{16}$, and $C_{16}H_{18}$) or *trans*-odd polyene radicals ($C_3H_5\cdot$, $C_5H_7\cdot$, $C_7H_9\cdot$, $C_9H_{11}\cdot$, $C_{11}H_{13}\cdot$, and $C_{13}H_{15}\cdot$). In alkali metal-doped complexes, each alkali atom is located at the vertex of the trigonal pyramid, whose basal triangle consists of an allylic group, $(CH)_3$. On the other hand, each chlorine atom is coplanar with the $(CH)_n$ chain and is connected with an allylic group by hydrogen bonding. The allylic group acts as a bidentate or tridentate ligand, forming an ionic closed-shell structure with the dopants. The molecular orbitals of the singly doped complexes are correlated with those of parent *trans*-polyene or odd polyene radical chains. The molecular orbitals of doubly doped complexes are analyzed on the basis of those of singly doped complexes. The molecular structure of the polson unit is presented, which is important for heavily doped polyacetylene to be metallic.

Polyacetylene changes from an insulator to a semiconductor and, finally, to a metallic conductor in the process of doping. Both an electron donor and acceptor can be used for doping. During the doping process charge-transfer occurs between the polyene chain and the dopant. Rice[1] as well as Su, Schrieffer, and Heeger[2] have suggested that the charged soliton is the product at the initial stage of doping. It is immobile because it is pinned adjacent to the ionized donor or acceptor. The charged soliton has a charge, but no spin. From a chemical structural view the charged soliton is modelled by a *trans*-odd polyene radical † combined with a dopant.

A polaron was proposed as a unit for metallic polyacetylene by Kivelson and Heeger.[3] A model of polaron may be a polyene molecule combined with a dopant, since it has a spin and a charge. However, a chain structure consisting of polaron units has not been fully studied from a chemical structural point of view. The structure of the combined chain of polaron units is dependent on the mode of combination.[4] Actually, the origin of the metallic state in heavily doped polyacetylene has not been well understood.[5,6]

We proposed that the charged species called a polson is a good candidate for a unit of metallic polyacetylene.[4,7,8] It has a spin and two charges, and has a symmetrical structure that is suitable as a repeating unit of the conducting chain.

The doped polyacetylene comprises a sequence of many short *trans*-$(CH)_n$ chains, each of which is coordinated by dopants.[9] In this regard, it is important to determine the molecular structure of the charge-transfer complexes of a short *trans*-$(CH)_n$ chain with a small number of dopants.

To elucidate the molecular and electronic structures of doped polyacetylene, fully optimized structures of model complexes were calculated by using ab initio RHF and UHF SCF MO methods. The model complexes are classified as follows:

(1) Models of a charged soliton in which a *trans*-odd polyene radical is coordinated by a univalent dopant atom,

(2) models of a polaron in which a *trans*-polyene is coordinated by a univalent dopant atom,

(3) models of a polson in which a *trans*-odd polyene radical is coordinated by two univalent dopant atoms from the same side, and

(4) models of a charged soliton-antisoliton pair and the central part of a polson-antipolson pair in which a neutral *trans*-polyene is coordinated by two univalent dopant atoms.

We discuss not only the geometries, but also the electronic structures of the complexes on the basis of the molecular orbitals, atomic charge densities and atomic spin densities. The energy band structure of the doped chain will be discussed in a succeeding paper.

Methods

We used the Gaussian 82[10] and the Gaussian 86[11] programs of the Institute for Molecular Science for ab initio RHF and UHF SCF MO calculations. The basis functions are 3-21G. The convergence limit for geometry optimization was set to CONVF=0.0003—0.001 in the Gaussian programs.

We first calculated the optimized geometry of (*Z*,*Z*)-$C_6H_8Li_2$ (**1**) using the 3-21G basis function, and compared the results with the experimental results of (*Z*,*Z*)-$C_6H_8Li_2(tmeda)_2$ determined by the X-ray method[12] (Table 1 and Fig. 1). The agreement between these two structures is quite satisfactory. We also compared the geometry of the allyl radical optimized by 3-21G to the molecular structure obtained from infrared diode laser spectroscopy;[13] the calculated values of the C–C distance and the C–C–C bond angle are 1.3884 Å and 124.30°, and the experimental values are 1.3869 Å and 123.96°, respectively. Accordingly, we believe that the optimized structures obtained by the

†The term 'odd-polyene radical' is used in this paper for a radical chain having the structural formula $-(CH)_{2n+1}\cdot-$.

RHF and UHF SCF MO calculation with the 3-21G basis function are reasonable for further studies of both closed- and open-shell systems. We used Na and Li atoms as electron donors and chlorine atoms as electron acceptors.

Results and Discussion

1. Class-(1) Complexes. Complexes of class-(1) comprise the (odd)-*trans*-polyene radical and a dopant atom. Both components are in the doublet spin state; accordingly, the complexes are either in the singlet or triplet state.

First of all, the optimized geometries of C_3H_5Li (**2**), C_3H_5Na (**3**) and C_3H_5Cl (**4**,**5**) were calculated, since they represent the basic structure of the doped polyacetylene. The geometries of **3** and **4** are illustrated in Fig. 2 and Table 2, where the dopant atom is located at the vertex of the trigonal pyramid, whose basal plane consists of C atoms of the allyl radical. The Cl complex of the allyl radical has another conformation, which is planar, as shown in Fig. 2 (C_3H_5Cl (**5**)). The conformation **5** is more stable than **4** by 0.023 eV in HF total energy due to the formation of hydrogen bonding.

The HOMO coefficients of **3**, **4**, and **5** are illustrated in Fig. 3, together with those of the dopant atoms in order to illustrate the molecular orbitals involved in the charge-transfer interaction. Since the three π-electrons of the allyl radical occupy α-HOMO, α-NHOMO, and β-HOMO, the electron in the α-HOMO is easily transferred to the acceptor atom; on the other hand, its β-LUMO can accept an electron from the donor atom. In the interaction of the β-LUMO of the allyl radical with the Na atom in **3**, the electron in the 3s orbital of the Na atom is promoted into the 3py orbital; then, the electron transfer occurs smoothly, since the phase of the 3py orbital matches that of the C2pz orbitals of the β-LUMO of the allyl group (Fig. 3a).

In the formation of complex **4**, the C2pz orbitals of α-HOMO of the allyl radical interacts with the 3py orbitals of the Cl atom (Fig. 3b). In complex **5**, the 3py and 3px orbitals of Cl (Figs. 3c and 3d) have matched phase with the H1s orbitals of the CH σ^* MO; accordingly, a back charge-transfer can occur through hydrogen bonding from the Cl 3px and 3py orbitals to the σ^* orbitals of the CH bonds.

In Fig. 4 the total atomic charges of **3**, **4**, **5** are illustrated. The amount of transferred charge to the Cl atom is larger in **5** than in **4**. Since almost all of the transferred charges are on C4 and C5 (Fig. 4), the Coulomb interaction between the dopant ion and the allylic group is most strong on these atoms. This is the major reason for bidentate coordination. In addition to the electrostatic Coulomb interaction, in complex **5** the hydrogen bonding between the Cl^- and the C4–H6 and C5–H7 also contributes to the stability of the complex. In the hydrogen-bonded system represented by X–H···Y, the charge-transfer interaction between the non-bonding orbital of the proton acceptor (Y) and the σ^* orbital of the X–H bond was found to be important in the formation of a hydrogen bond.[14] The complexes **2**—**5** have a closed-shell electronic structure. They comprise the allylic ion and a dopant. This pair is denoted **A** in the following discussion in order to illustrate the chain structure in compact form.

Next, complexes C_5H_7Na (**6**) and C_5H_7Cl (**7**) were calculated to find the optimized geometries and molecular orbitals which will be used in a later discussion. The total atomic charges of **6** and **7** are shown in Fig. 4.

Odd polyene radicals that are longer than C_3H_5 have more than one site to which the dopant can coordinate (Fig. 5). The location of the **A** unit in the chain determines the spin state of the resultant complex. As shown in Fig. 5, the carbon atoms of an odd-$(CH)_n$ chain can be divided into two sets, (starred and unstarred), such

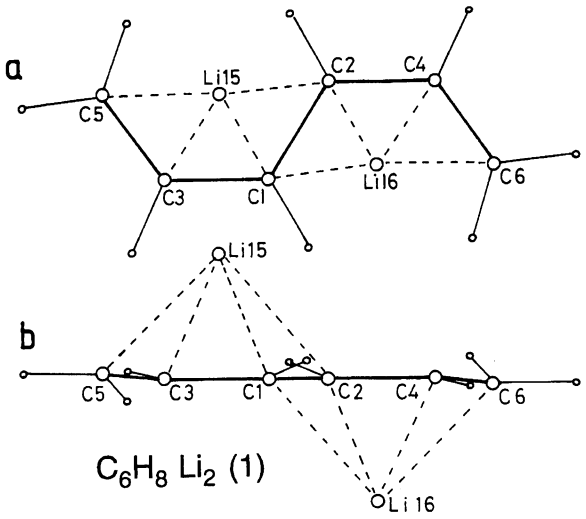

Fig. 1. Optimized molecular geometry of (*Z*,*Z*)-$C_6H_8Li_2$ (**1**), (a) projected onto the best plane of (*Z*,*Z*)-C_6H_8, (b) projected onto the plane perpendicular to it.

Table 1. Optimized Geometrical Parameters of (*Z*,*Z*)-$C_6H_8Li_2$ Compared with the Experimental Values of (*Z*,*Z*)-$C_6H_8Li_2(tmeda)_2$[12]

(*Z*,*Z*)-$C_6H_8Li_2$ (**1**) Molecular symmetry	C_i	
Atomic distance (Å)	Calculated	Experiment
C2–C1	1.491	1.456
C3–C1	1.399	1.378
C5–C3	1.391	1.363
Li15–C2	2.194	2.404
Li15–C1	2.102	2.263
Li15–C3	2.151	2.210
Li15–C5	2.255	2.269
Bond angle (deg.)		
∠C3–C1–C2	121.9	123.7
∠C5–C3–C1	126.3	130.1

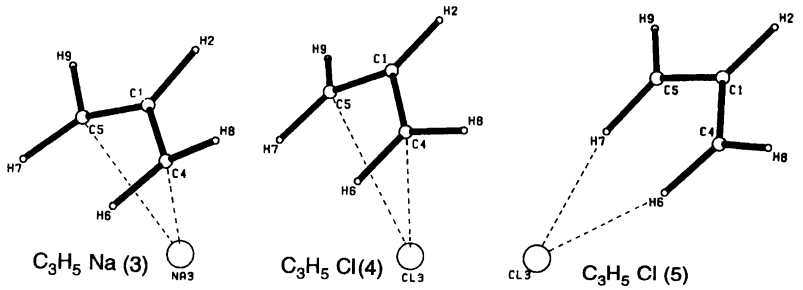

Fig. 2. Optimized molecular geometries of C_3H_5Na (**3**), C_3H_5Cl (**4**), and C_3H_5Cl (**5**).

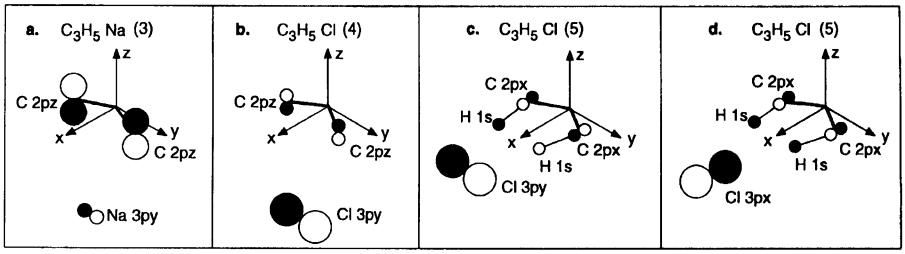

Fig. 3. Shematic representation of the MO's concerned with a charge-transfer interaction in the coordination region.

Table 2. Optimized Geometrical Parameters of C_3H_5Li (**2**), C_3H_5Na (**3**), C_3H_5Cl (**4**), and C_3H_5Cl (**5**) The representation of dihedral angles are illustrated in the figure, which is used in other tables.

Basis set 3-21G	$(C_3H_5)Li$(**2**)	$(C_3H_5)Na$(**3**)	$(C_3H_5)Cl$(**4**)	$(C_3H_5)Cl$(**5**)
Molecular symmetry	Cs	Cs	Cs	C_{2v}
Total energy (HF) (Hartree)	−123.22822	−276.67014	−573.06647	−573.06730
Atomic distance (Å)				
Dp3–C1	2.098	2.427	2.983	3.745
Dp3–C4	2.145	2.475	2.758	3.248
Dp3-H6	2.444	2.725	2.664	2.248
C4–C1	1.394	1.393	1.371	1.373
H2–C1	1.080	1.082	1.070	1.071
H6–C4	1.083	1.082	1.069	1.089
H8–C4	1.072	1.073	1.072	1.074
Bond Angle (deg.)				
∠Dp3–C1-H2	119.59	117.65	121.44	180.00
∠Dp3–C1–C4	72.65	75.40	67.20	58.60
∠C4–C1-H2	116.43	115.71	120.35	121.40
∠C4–C1–C5	125.97	128.09	116.57	117.19
∠H6–C4–C1	119.08	118.93	121.88	119.31
∠H8–C4–C1	119.89	119.86	121.16	120.90
Torsion Angle (deg.)				
C4–C1(H2)-Dp3	84.22	86.35	80.31	—
H6–C4–C1–C5	−28.56	−23.41	−20.53	0.00
H8–C4–C1–C5	178.71	184.05	161.83	180.00

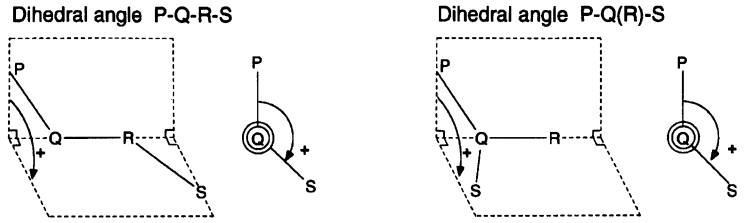

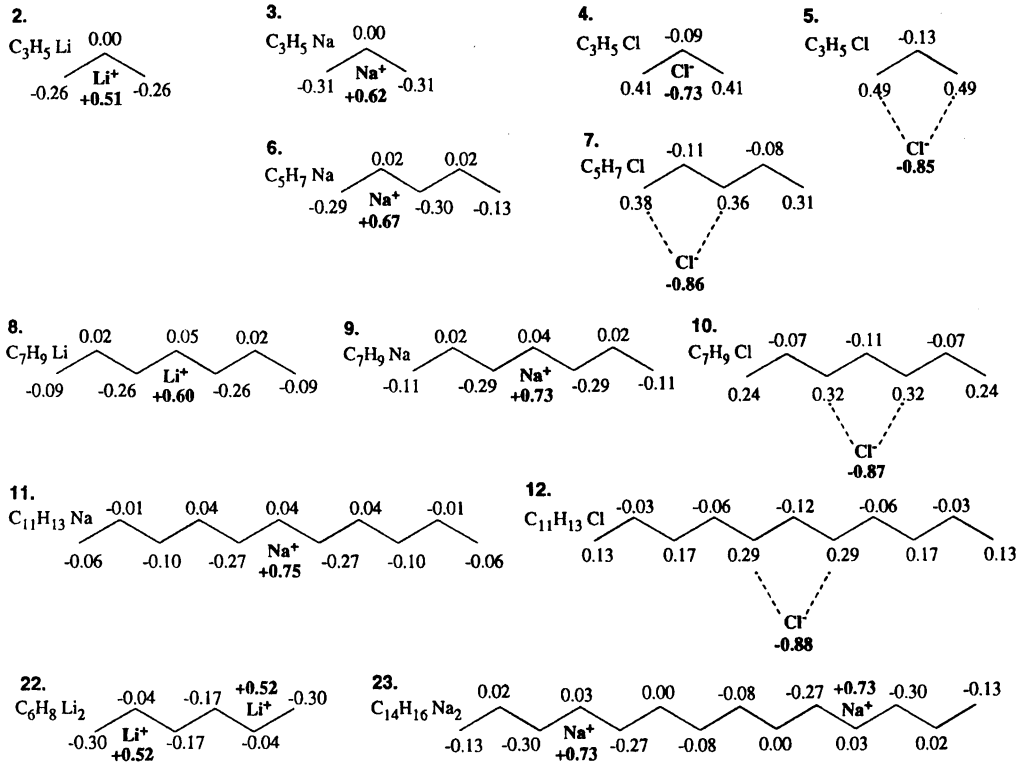

Fig. 4. Total atomic charges with hydrogens summed into carbon atoms. The number of complexes is mentioned in the text.

that no two members of the same set are bonded together (Fig. 5).[15] If the two adjoining starred carbon atoms are ligating atoms in the **A** group, the product is a singlet complex, since each carbon chain on both sides of the **A** group contains an even number of carbon atoms. On the other hand, if the two adjoining unstarred carbon atoms are ligating atoms in the **A** group, the product is a triplet complex, since an odd number of carbon atoms exist on both sides of the **A** group. To find the structure of the charged soliton, we calculated the model compounds of the singlet complexes as follows: C_7H_9Li (**8**), C_7H_9Na (**9**), and $C_{11}H_{13}Na$ (**11**) where C_s symmetry was assumed, and C_7H_9Cl (**10**), and $C_{11}H_{13}Cl$ (**12**) where C_{2v} symmetry was assumed.

In contrast to C_3H_5Cl (**4**), only the planar conformation was obtained in the Cl complex of C_7H_9. Therefore, the planar conformation was assumed in the calculation of $C_{11}H_{13}Cl$ (**12**). The optimized geometries of $C_{11}H_{13}Na$ (**11**) and $C_{11}H_{13}Cl$ (**12**) are shown in Table 3. For the other complexes, the geometrical parameters of the coordination regions are summarized in Table 8.

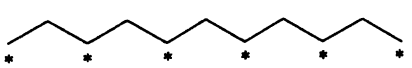

Fig. 5. Starred and unstarred carbon atoms of the odd-polyene radical. The carbon atoms of an odd polyene radical chain are divided into two sets, (starred and unstarred), such that no two members of the same set are bonded together.[15]

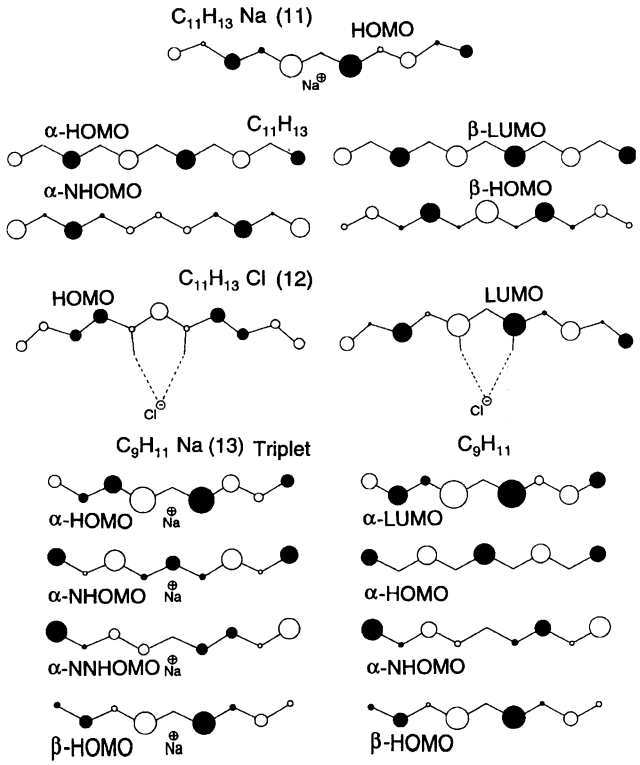

Fig. 6. HOMO coefficients of class-(1) complexes; $C_{11}H_{13}Na$ (**11**) (top), $C_{11}H_{13}Cl$ (**12**) (middle), and triplet $C_9H_{11}Na$ (**13**) (bottom) comparing with MO coefficients of related orbitals of $C_{11}H_{13}$ and C_9H_{11}. The black and white circles represent the relative values and the signs of the coefficients of the π-orbitals.

Table 3. Optimized Geometrical Parameters and the Projection of $C_{11}H_{13}Na$ (**11**) and $C_{11}H_{13}Cl$ (**12**). Dopant atoms, Na and Cl, are expressed as 'Dp' in the Table. (a) The geometry projected onto the best plane of $C_{11}H_{13}$, (b) projected onto the plane perpendicular to it.

	$C_{11}H_{13}Na$(**11**)	$C_{11}H_{13}Cl$(**12**)	Basis set
Molecular symmetry	C_s	C_{2v}	3-21G
Total energy (HF) (Hartree)	−582.51585	−878.95326	

Atomic distance (Å)			Bond angle (deg.)			Dihedral angle (deg.)	
	$C_{11}H_{13}Na$	$C_{11}H_{13}Cl$		$C_{11}H_{13}Na$	$C_{11}H_{13}Cl$		$C_{11}H_{13}Na$
Dp3–C1	2.449	3.868					
Dp3–C4	2.524	3.363	∠Dp3–C1–C4	76.74	58.61		
Dp3-H14		2.337	∠Dp3–C1-H2	115.83	180.00	Dp3–C1(H2)–C4	−87.32
			∠C4–C1-H2	116.08	121.39		
C4–C1	1.391	1.379	∠C4–C1–C5	127.59	117.22	H2–C1–C4–C6	4.13
C6–C4	1.442	1.419	∠C6–C4–C1	122.84	125.89	C6–C4–C1–C5	178.04
C8–C6	1.338	1.344	∠C8–C6–C4	127.13	119.23	C8–C6–C4–C1	173.59
C10–C8	1.456	1.450	∠C10–C8–C6	123.44	124.61	C10–C8–C6–C4	179.22
C12–C10	1.325	1.325	∠C12–C10–C8	125.56	122.10	C12–C10–C8–C6	180.24
H2–C1	1.083	1.073					
H14–C4	1.083	1.083	∠H14–C4–C1	118.44	116.38	H14–C4–C1–C5	−16.19
H16–C6	1.081	1.074	∠H16–C6–C4	115.38	119.88	H16–C6–C4–C1	−6.73
H18–C8	1.077	1.077	∠H18–C8–C6	119.77	118.41	H18–C8–C6–C4	−1.63
H20–C10	1.078	1.074	∠H20–C10–C8	115.65	117.31	H20–C10–C8–C6	0.47
H22–C12	1.075	1.074	∠H22–C12–C10	121.75	121.78	H22–C12–C10–C8	−0.02
H24–C12	1.073	1.072	∠H24–C12–C10	121.76	121.64	H24–C12–C10–C8	180.32

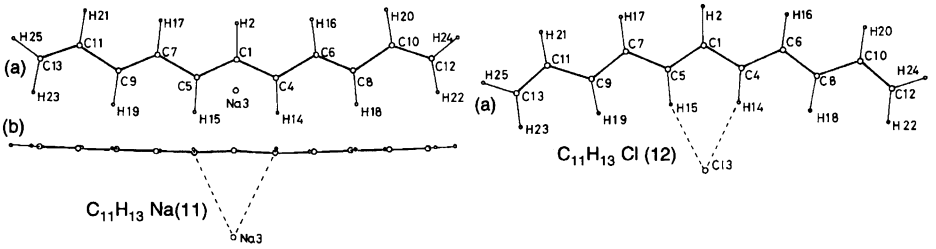

The total atomic charges shown in Fig. 4 indicate that the charge transfer occurs effectively, and that the total charge on the chain is larger in Cl complexes (p-doping) than Na or Li complexes (n-doping). The excess charge is distributed over the starred carbon atoms (Fig. 5), and is more extended in the p-doped chain than in the n-doped chain. However, most of the charge remains in the central **A** region in both types of complexes. The charge distributions in the **A** region of **6**, **9** and **11** are almost the same as that of **3**, and those in the **A** region of **7**, **10**, and **12** are almost the same as that of **5**. This means that the $-(CH)_3X-$ (X=Na, Li, and Cl) group in the chain is a stable unit.

The molecular structure of the chain is deformed due to the electron transfer. Most of the bond lengths are longer, in $C_{11}H_{13}Na$ (**11**) than in $C_{11}H_{13}Cl$ (**12**) because more electrons exist on the $C_{11}H_{13}$ chain of the former (Table 3). In **11** the Na atom is located at the vertex of the trigonal pyramid, as was found in **2**, **3**, **6**, and **9**. The bond alternation is clearly shown in Table 3 in the carbon chains of C6–C8–C10–C12 and C7–C9–C11–C13. The central **A** group is connected to these conjugated double bonds at both sides by the single bonds. If symbol **E** represents polyene comprising an even number of carbon atoms, the complex is expressed as **E**–**A**–**E**. In general, the chain lengths of **E**'s are not necessarily the same, since the dopant can react to any two adjoining starred carbon atoms of the chain. The patterns of the bond alternation in both **E** groups are symmetrical with respect to the plane of symmetry of **A** group. The chain structure, **E**–**A**–**E**, corresponds to the molecular structure of a unit of the so-called charged soliton chain.

The MO coefficients of $C_{11}H_{13}$, **11** and **12** are illustrated in Fig. 6. The HOMO coefficients of **11** is almost the same as those of the α-HOMO and the β-LUMO of $C_{11}H_{13}$; this indicates that charge-transfer occurs to the β-LUMO of $C_{11}H_{13}$ in n-doping. The HOMO coefficients of **12** show the pattern of superposition of β-HOMO and α-NHOMO of $C_{11}H_{13}$, since the electron is removed from the α-HOMO of $C_{11}H_{13}$. The coefficients of LUMO of **12** represent the population of hole.

The pattern of the HOMO of **11** and the LUMO of **12** in the **A** region are almost the same as those of the allylic anion and cation, respectively. The excess charge, either electrons or holes, is localized in the **A** group, and the Coulomb attraction between the excess charge and the dopant ion is most significant.

Table 4. Optimized Geometrical Parameters and the Projection of $C_{12}H_{14}Na$ (**17**) and $C_{12}H_{14}Cl$ (**18**). Dopant atoms, Na and Cl, are expressed as 'Dp' in the Table. (a) The geometry projected onto the best plane of $C_{12}H_{14}$, (b) projected onto the plane perpendicular to it.

		$C_{12}H_{14}Na$(**17**)	$C_{12}H_{14}Cl$(**18**)	Basis set
Molecular symmetry		C_1	C_s	3-21G
Total energy (HF) (Hartree)		−620.76688	−917.20272	
Atomic distance (Å)		Bond Angle (deg.)		Dihedral angle (deg.)	
	$C_{12}H_{14}Na$	$C_{12}H_{14}Cl$		$C_{12}H_{14}Na$	$C_{12}H_{14}Cl$		$C_{12}H_{14}Na$
Dp27–C2	2.392	3.824					
Dp27–C1	2.600	3.354	∠Dp27–C2–C1	81.95	60.05	Dp27–C2(H14)–C1	90.76
Dp27–C4	2.556	3.337	∠Dp27–C2–C4	79.95	59.34	Dp27–C2(H14)–C4	−88.31
Dp27-H13		2.348	∠Dp27–C2-H14	109.29	179.62		
Dp27-H16		2.324					
C12–C11	1.367	1.368	∠C12–C11–C7	124.49	123.60	C12–C11–C7–C5	179.94
C11–C7	1.420	1.417	∠C11–C7–C5	124.00	123.16	C11–C7–C5–C3	179.95
C7–C5	1.394	1.395	∠C7–C5–C3	124.67	123.56	C7–C5–C3–C1	180.83
C5–C3	1.401	1.394	∠C5–C3–C1	124.92	121.17	C5–C3–C1–C2	181.22
C3–C1	1.409	1.400	∠C3–C1–C2	125.89	123.49		
C2–C1	1.406	1.386					
C4–C2	1.409	1.386	∠C4–C2–C1	125.80	119.39	C4–C2–C1–C3	185.34
C6–C4	1.415	1.403	∠C6–C4–C2	125.40	123.78	C6–C4–C2–C1	176.61
C8–C6	1.386	1.380	∠C8–C6–C4	125.63	120.81	C8–C6–C4–C2	176.77
C9–C8	1.424	1.423	∠C9–C8–C6	124.13	123.66	C9–C8–C6–C4	179.40
C10–C9	1.364	1.362	∠C10–C9–C8	124.89	122.95	C10–C9–C8–C6	179.92
H26–C12	1.073	1.072	∠H26–C12–C11	121.52	121.33	H26–C12–C11–C7	180.12
H25–C12	1.074	1.074	∠H25–C12–C11	121.43	121.49	H25–C12–C11–C7	−0.13
H24–C11	1.077	1.075	∠H24–C11–C7	116.92	117.41	H24–C11–C7–C5	0.07
H19–C7	1.077	1.076	∠H19–C7–C5	118.45	118.73	H19–C7–C5–C3	−0.48
H17–C5	1.079	1.075	∠H17–C5–C3	117.42	117.64	H17–C5–C3–C1	1.25
H15–C3	1.080	1.076	∠H15–C3–C1	117.57	119.64	H15–C3–C1–C2	0.25
H13–C1	1.084	1.082	∠H13–C1–C2	117.24	116.85	H13–C1–C2–C4	9.73
H14–C2	1.082	1.076	∠H14–C2–C1	117.24	120.33	H14–C2–C1–C3	4.33
			∠H14–C2–C4	116.96	120.28	H14–C2–C4–C6	−2.38
H16–C4	1.084	1.083	∠H16–C4–C2	117.38	116.76	H16–C4–C2–C1	−10.77
H18–C6	1.080	1.075	∠H18–C6–C4	116.90	119.66	H18–C6–C4–C2	−2.67
H20–C8	1.078	1.076	∠H20–C8–C6	118.58	118.04	H20–C8–C6–C4	−1.35
H21–C9	1.077	1.075	∠H21–C9–C8	116.75	117.73	H21–C9–C8–C6	0.18
H22–C10	1.075	1.073	∠H22–C10–C9	121.45	121.40	H22–C10–C9–C8	−0.18
H23–C10	1.073	1.072	∠H23–C10–C9	121.57	121.38	H23–C10–C9–C8	180.27

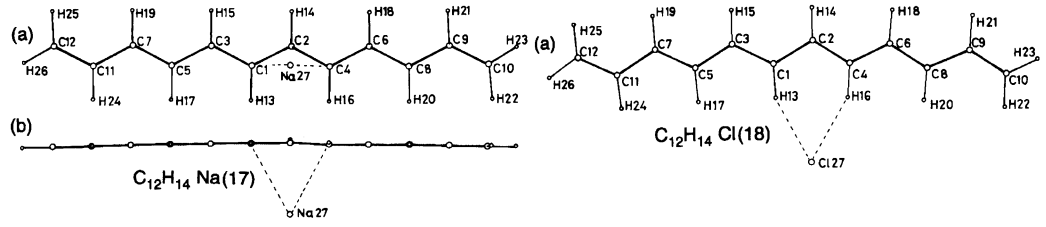

Next, the optimized geometry of $C_9H_{11}Na$ (**13**) was calculated as a model complex in the triplet state, assuming C_s symmetry. The dopant is coordinated by the allylic unit in the center of the chain. The **A** group is formed in the center by coordination at two unstarred carbon atoms (Fig. 5), and is connected to two allylic radicals at both ends of the chain. As shown in Fig. 7, the sum of the spin population in the **A** group is almost zero; effective spin densities, however, exist in the allylic groups at both ends, while excess charge does not exist in these groups. This indicates that the chain is expressed as **O–A–O**, where the symbol "**O**" represents a chain comprising an odd number of carbon atoms. In general, the chain lengths of **O**'s in **O–A–O** are not necessarily the same.

The large spin population on both **O** groups clearly shows that the original radical chain is changed to a complex chain containing two allylic radical chains at both ends.

The MO coefficients of the α-HOMO of $C_9H_{11}Na$ (**13**) indicates that n-doping occurs in the α-LUMO of C_9H_{11} (Fig. 6). The correspondence between the MO

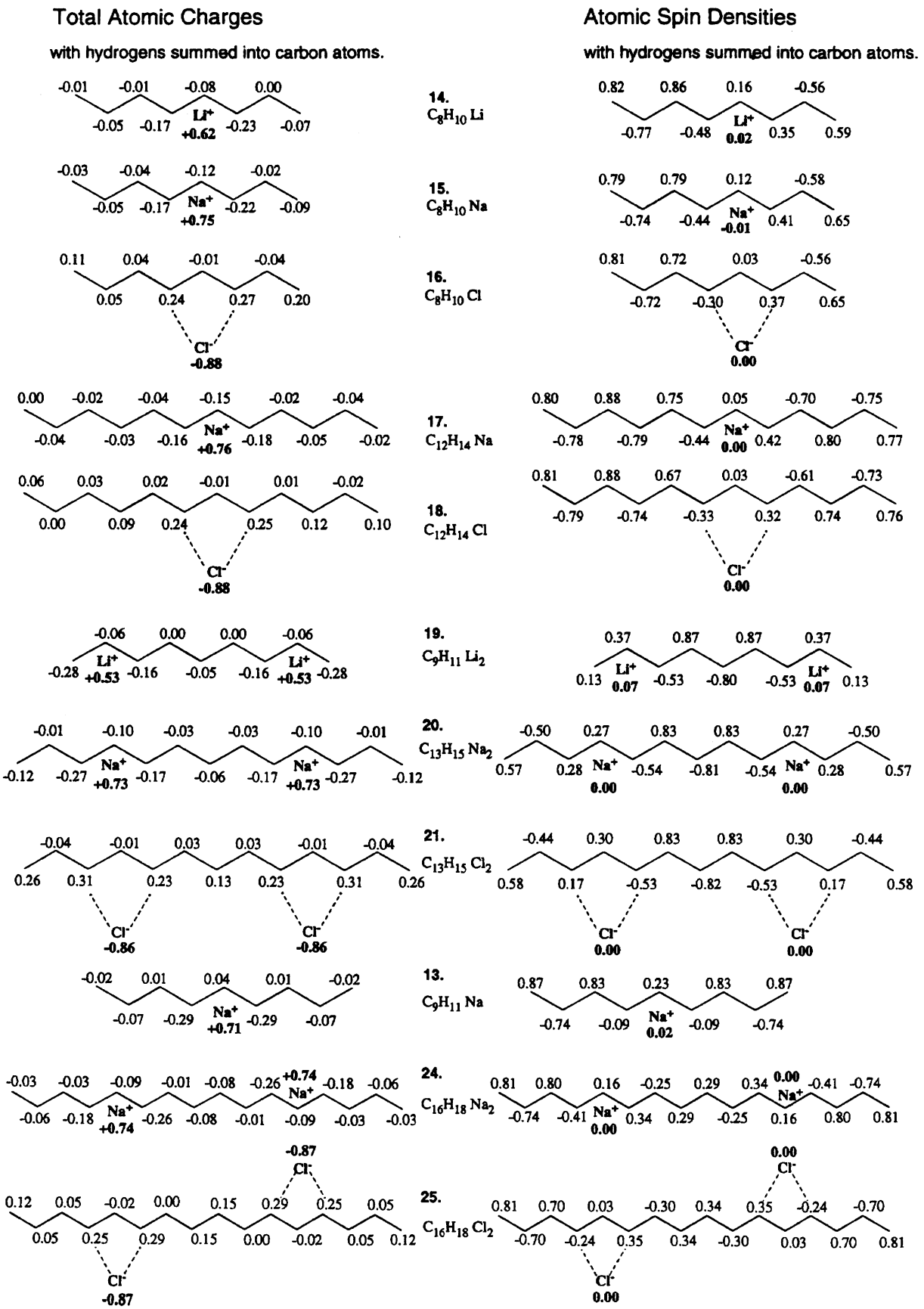

Fig. 7. Total atomic charges and atomic spin densities with hydrogens summed into carbon atoms. The number of complexes is mentioned in the text.

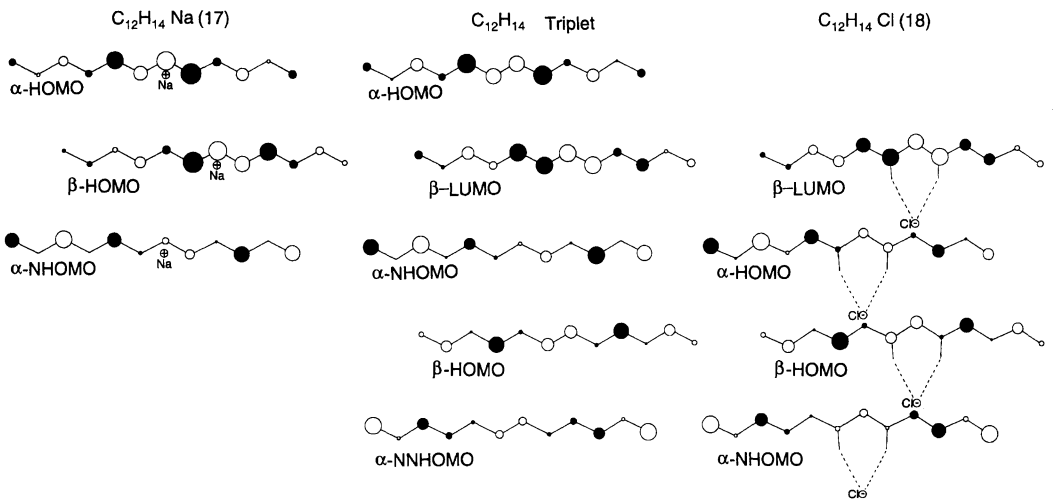

Fig. 8. Comparison of the MO coefficients of $C_{12}H_{14}Na$ (**17**) (left), $C_{12}H_{14}Cl$ (**18**) (right), and $C_{12}H_{14}$ (triplet) (center).

of the reactant and the product is extremely good, since they are both open-shell systems, and the electron correlation is properly taken into account in the UHF MO calculation.

2. Class-(2) Complexes. The class-(2) complex comprises a neutral polyene and a dopant atom; accordingly, the complex is in the doublet state. The molecular orbitals were calculated on $C_8H_{10}Li$ (**14**), $C_8H_{10}Na$ (**15**), $C_8H_{10}Cl$ (**16**), $C_{12}H_{14}Na$ (**17**), and $C_{12}H_{14}Cl$ (**18**). The optimized geometries of $C_{12}H_{14}Na$ (**17**) and $C_{12}H_{14}Cl$ (**18**) are shown in Table 4. A planar conformation was assumed for $C_{12}H_{14}Cl$ (**18**) following the results of $C_{11}H_{13}Cl$ (**12**). The total atomic charges and the atomic spin densities of these complexes are illustrated in Fig. 7. In the Na complex, the total atomic charge on the C2 atom is larger than that in the case of the class-(1) complex. This shows that the allylic group acts as a tridentate ligand in the class-(2) complex.

The geometries, the total atomic charges in the coordination region, C1–C2–C4, are in fairly good agreement with those of the **A** region of class-(1) complexes. The sum of the atomic spin densities in this region is almost zero (Fig. 7). This shows that the allylic group and the dopant forms a similar stable closed shell to those found in class-(1) complexes, which is represented as **A**. On the right side of **A**, conjugated double bonds are formed with an even number of carbon atoms, (–C6–C8–C9–C10), as represented by **E**. The **E** and **A** combine to form a closed-shell structure with ca. 80 percent of the total excess charge. On the left side of **A**, a radical chain is formed with an odd number of carbon atoms, (C12–C11–C7–C5–C3–), which keeps ca. 80 percent of sum of the atomic spin densities (Fig. 7). Accordingly, the complexes, $(C_{12}H_{14})^-Na^+$(**17**) and $(C_{12}H_{14})^+Cl^-$(**18**), are represented as **O–A–E**, which comprise the radical part **O**, $-C_5H_6$, and the ionic closed-shell part **A–E**, $-(C_7H_8)^-Na^+$, and $-(C_7H_8)^+Cl^-$, respectively.

The MO's of the charge-transfer complexes are compared with those of triplet $C_{12}H_{14}$ in Fig. 8. The α-HOMO, β-HOMO, and α-NHOMO of **17** are closely correlated to the α-HOMO, β-LUMO, and α-NHOMO of triplet $C_{12}H_{14}$, respectively. Similarly, the α-HOMO, β-HOMO, and α-NHOMO of **18** are closely correlated to the α-NHOMO, β-HOMO, and α-NNHOMO of triplet $C_{12}H_{14}$. If an electron is transferred from the α-HOMO of triplet $C_{12}H_{14}$ to the Cl atom, the α-HOMO becomes empty, and the α-NHOMO, β-HOMO and α-NNHOMO of $C_{12}H_{14}$ become the α-HOMO, β-HOMO and α-NHOMO of **18**. On the other hand, the β-LUMO of triplet $C_{12}H_{14}$ becomes the β-HOMO of **17** by receiving an electron from the Na atom. The α-HOMO's of **17** and $C_{12}H_{14}$ have the same pattern, since their origin are common. This close correlation found between the MO coefficients of the complex and the polyene in the triplet state does not necessarily mean that the actual charge transfer proceeds via the triplet state of polyene. However, the MO calculation on the polyene-dopant system showed that a charge-transfer cannot occur in a chain with a structure optimized with the singlet polyene, which has normal conjugated double bonds. On the other hand, the chain of triplet polyene comprises two radical parts; if one of them reacts with the dopant to form **A** and the other remains as **O**, a class-(2) complex is formed. On the basis of these results, it is considered that a charge-transfer reaction occurs in polyene with a deformed conformation whose structure is very close to those found in the triplet state.

3. Class-(3) Complexes. In the above disccusion concerning class-(1) and -(2) complexes, group **A** has a closed-shell electronic structure. Three chain structures, **E–A–E′**, **O–A–O′**, and **E–A–O**, cover all types of chain sequences in a singly-doped $(CH)_n$ chain. In the following sections we discuss the structures of doubly doped systems.

A class-(3) complex comprises a *trans*-odd polyene radical and two univalent dopant atoms, in which each dopant atom is coordinated by a set of two adjoining starred carbon atoms (Fig. 5), such that at least one

Table 5. Optimized Geometrical Parameters and the Projection of $C_{13}H_{15}Na_2$ (**20**) and $C_{13}H_{15}Cl_2$ (**21**). Dopant atoms, Na and Cl, are expressed as 'Dp' in the Table. (a) The geometry projected onto the best plane of $C_{13}H_{15}$, (b) projected onto the plane perpendicular to it.

		$C_{13}H_{15}Na_2$(**20**)	$C_{13}H_{15}Cl_2$(**21**)	Basis set
Molecular symmetry		*Cs*	*C2v*	3-21G
Total energy (HF) (Hartree)		−819.81901	−1412.67550	
Atomic distance (Å)		Bond angle (deg.)		Dihedral angle (deg.)	
	$C_{13}H_{15}Na_2$	$C_{13}H_{15}Cl_2$		$C_{13}H_{15}Na_2$	$C_{13}H_{15}Cl_2$		$C_{13}H_{15}Na_2$
Dp29–C5	2.644	3.411					
Dp29–C7	2.406	3.790	∠Dp29–C7–C5	83.56	63.73		
Dp29–C9	2.449	3.215	∠Dp29–C7–C9	74.70	55.57	Dp29–C7(H19)–C5	93.83
Dp29-H17		2.447	∠Dp29–C7-H19	111.96	175.88	Dp29–C7(H19)–C9	−83.38
Dp29-H21		2.169					
C3–C1	1.399	1.398	∠C3–C1–C4	124.95	121.52	C3–C1(H2)–C4	−182.13
C5–C3	1.419	1.409	∠C5–C3–C1	125.06	122.98	C5–C3–C1-H2	0.54
C7–C5	1.399	1.385	∠C7–C5–C3	125.48	121.90	C7–C5–C3–C1	184.32
C9–C7	1.417	1.393	∠C9–C7–C5	126.53	119.30	C9–C7–C5–C3	183.40
C11–C9	1.434	1.410	∠C11–C9–C7	123.70	124.44	C11–C9–C7–C5	179.10
C13–C11	1.354	1.358	∠C13–C11–C9	127.31	119.11	C13–C11–C9–C7	172.94
H2–C1	1.080	1.075	∠H2–C1–C3	117.50	119.24		
H15–C3	1.080	1.076	∠H15–C3–C1	117.65	118.47	H15–C3–C1-H2	182.74
H17–C5	1.085	1.082	∠H17–C5–C3	116.77	120.65	H17–C5–C3–C1	−2.49
			∠H17–C5–C7	117.42	117.45	H17–C5–C7–C9	10.24
H19–C7	1.082	1.075	∠H19–C7–C5	116.64	120.39	H19–C7–C5–C3	0.30
			∠H19–C7–C9	116.77	120.31	H19–C7–C9–C11	2.20
H21–C9	1.084	1.088	∠H21–C9–C7	117.69	116.60	H21–C9–C7–C5	−16.39
H23–C11	1.082	1.074	∠H23–C11–C9	115.41	120.13	H23–C11–C9–C7	−6.72
H25–C13	1.076	1.074	∠H25–C13–C11	121.67	120.57	H25–C13–C11–C9	−1.73
H27–C13	1.073	1.072	∠H27–C13–C11	121.46	121.61	H27–C13–C11–C9	180.20

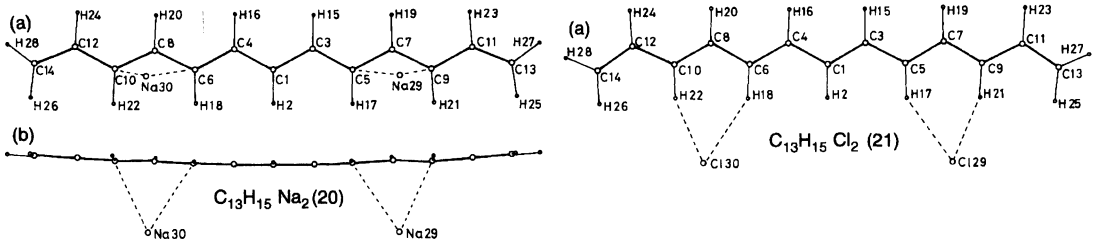

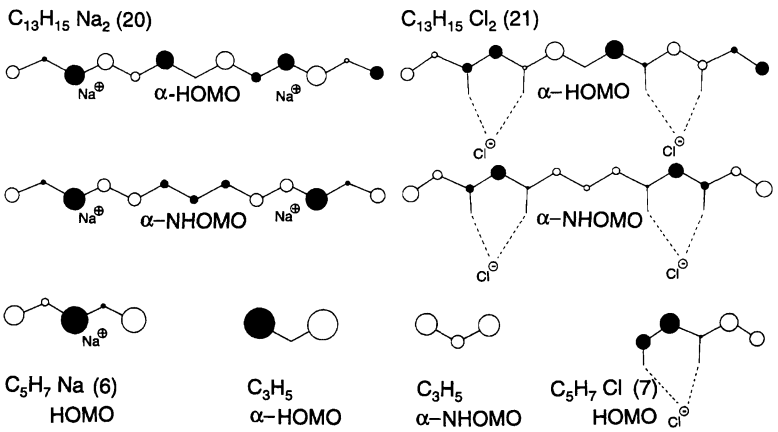

Fig. 9. α-HOMO coefficients of class (3) complexes; $C_{13}H_{15}Na_2$ (**20**) (left) and $C_{13}H_{15}Cl_2$ (**21**) (right), showing the patterns of HOMO's of n-doped and p-doped polson units. These patterns are explained using the HOMO coefficients of C_5H_7Na (**6**) and C_5H_7Cl (**7**), and α-HOMO and α-NHOMO coefficients of C_3H_5.

Table 6. Optimized Geometrical Parameters and the Projection of $C_{14}H_{16}Na_2$ (**23**). (a) The geometry projected onto the best plane of $C_{14}H_{16}$, (b) projected onto the plane perpendicular to it.

$C_{14}H_{16}Na_2$(**23**)				Basis set	
Molecular symmetry			C_i	3-21G	
Total energy (HF)(Hartree)			−858.04415		
Atomic distance (Å)		Bond angle (deg.)		Dihedral angle (deg.)	
Na31–C5	2.534	∠Na31–C7–C5	77.74		
Na31–C7	2.437	∠Na31–C7–C9	75.49		
Na31–C9	2.488	∠Na31–C7-H21	115.89	Na31–C7(H21)–C5	−88.51
				Na31–C7(H21)–C9	85.72
C2–C1	1.455				
C3–C1	1.337	∠C3–C1–C2	124.76	C3–C1–C2–C4	180.00
C5–C3	1.450	∠C5–C3–C1	126.79	C5–C3–C1–C2	178.98
C7–C5	1.384	∠C7–C5–C3	123.42	C7–C5–C3–C1	174.67
C9–C7	1.401	∠C9–C7–C5	127.91	C9–C7–C5–C3	176.50
C11–C9	1.448	∠C11–C9–C7	122.42	C11–C9–C7–C5	−179.63
C13–C11	1.331	∠C13–C11–C9	127.68	C13–C11–C9–C7	−170.30
H15–C1	1.079	∠H15–C1–C3	118.97	H15–C1–C3–C5	−1.31
H17–C3	1.081	∠H17–C3–C5	115.40	H17–C3–C5–C7	−5.62
H19–C5	1.084	∠H19–C5–C7	118.48	H19–C5–C7–C9	−15.71
H21–C7	1.083	∠H21–C7–C5	115.99	H21–C7–C5–C3	3.10
		∠H21–C7–C9	115.81	H21–C7–C9–C11	−6.21
H23–C9	1.083	∠H23–C9–C7	118.13	H23–C9–C7–C5	18.61
H25–C11	1.082	∠H25–C11–C9	114.84	H25–C11–C9–C7	9.85
H27–C13	1.076	∠H27–C13–C11	121.84	H27–C13–C11–C9	1.62
H29–C13	1.073	∠H29–C13–C11	121.57	H29–C13–C11–C9	−179.66

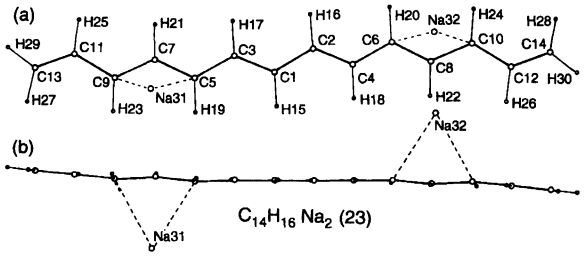

starred carbon atom remains between the sets. The molecular orbitals of $C_9H_{11}Li_2$ (**19**), $C_{13}H_{15}Na_2$ (**20**), and $C_{13}H_{15}Cl_2$ (**21**) were calculated assuming C_s symmetry for the two former and C_{2v} symmetry for the latter. The optimized geometries of $C_{13}H_{15}Na_2$ (**20**) and $C_{13}H_{15}Cl_2$ (**21**) are shown in Table 5.

The total atomic charges and atomic spin densities are illustrated in Fig. 7. The values of the geometrical parameters in the coordination region, C5–C7–C9 and C6–C8–C10, are in good agreement with those of **A** group in the class-(1) and -(2) complexes. This confirms that the allylic groups and the dopants form similar stable closed-shells to that of the **A** groups found in the class-(1) and -(2) complexes. The sum of the atomic spin densities shows that the $(CH)_3$ group in the center, C3–C1–C4, maintains an unpaired electron; consequently, it is regarded as being an allylic radical, **O**. Accordingly, the complexes are represented as **E–A–O–A–E**, and are in the doublet spin state.

The MO's of $C_{13}H_{15}Na_2$ (**20**) and $C_{13}H_{15}Cl_2$ (**21**) are compared with those of the allyl group, C_5H_7Na (**6**) and C_5H_7Cl (**7**) in view of finding a relation between them (Fig. 9). The α-HOMO of **20** comprises an antisymmetric combination of HOMO's of **6** and the α-HOMO of the allyllic radical. In contrast, the α-NHOMO is a symmetric combination of the HOMO's of **6** and the α-NHOMO of the allyllic radical. Similarly, the α-HOMO of **21** is an antisymmetric combination of the HOMO's of **7** and the α-HOMO of the allyllic radical. The α-NHOMO of **21** is a symmetric combination of the HOMO's of **7** and the α-NHOMO of the allyllic radical. The pattern of α-HOMO of the allyllic radical appears in both the α-HOMO of **20** and the α-HOMO of **21**.

The above-mentioned result indicates that the original uniform chain of $C_{13}H_{15}$ is changed into a mixed structure comprising two **A** units and a **O** unit, and two **E** units at both ends, namely an **E–A–O–A–E** chain, is formed. This chain structure is called the "**polson**" structure. Group **A** plays the role of partition between the **E** and **O** groups.

On the basis of the above discussion, heavily doped

Table 7. Optimized Geometrical Parameters and the Projection of $C_{16}H_{18}Na_2$ (triplet) (**24**) and $C_{16}H_{18}Cl_2$(triplet) (**25**). Dopant atoms, Na and Cl, are expressed as 'Dp' in the Table. (a) The geometry projected onto the best plane of $C_{16}H_{18}$, (b) projected onto the plane perpendicular to it.

	$C_{16}H_{18}Na_2$(**24**)	$C_{16}H_{18}Cl_2$(**25**)	Basis set
Molecular symmetry	C_i	C_i	3-21G
Total energy (HF) (Hartree)	−934.49986	−1527.36792	

Atomic distance (Å)			Bond angle (deg.)			Dihedral angle (deg.)		
	$C_{16}H_{18}Na_2$	$C_{16}H_{18}Cl_2$		$C_{16}H_{18}Na_2$	$C_{16}H_{18}Cl_2$		$C_{16}H_{18}Na_2$	$C_{16}H_{18}Cl_2$
Dp35–C5	2.474	3.283						
Dp35–C7	2.412	3.831	∠Dp35–C7–C5	75.64	56.73			
Dp35–C9	2.629	3.394	∠Dp35–C7–C9	82.67	61.43	Dp35–C7(H23)–C5	−83.92	0.0
Dp35-H21		2.245	∠Dp35–C7-H23	110.91	177.79	Dp35–C7(H23)–C9	92.22	180.0
Dp35-H25		2.399						
C2–C1	1.465	1.461						
C3–C1	1.342	1.345	∠C3–C1–C2	124.57	123.10	C4–C2–C1–C3	180.00	180.0
C5–C3	1.444	1.425	∠C5–C3–C1	127.20	118.99	C5–C3–C1–C2	178.36	180.0
C7–C5	1.411	1.382	∠C7–C5–C3	123.09	125.29	C7–C5–C3–C1	173.83	180.0
C9–C7	1.397	1.385	∠C9–C7–C5	126.69	118.16	C9–C7–C5–C3	178.13	180.0
C11–C9	1.414	1.402	∠C11–C9–C7	125.68	123.61	C11–C9–C7–C5	185.24	180.0
C13–C11	1.410	1.404	∠C13–C11–C9	124.57	121.34	C13–C11–C9–C7	−177.72	179.83
C15–C13	1.374	1.374	∠C15–C13–C11	125.19	123.09	C15–C13–C11–C9	−179.04	180.14
H17–C1	1.079	1.076	∠H17–C1–C3	119.14	119.12	H17–C1–C3–C5	−1.36	0.0
H19–C3	1.082	1.074	∠H19–C3–C5	115.31	120.12	H19–C3–C5–C7	−6.69	0.0
H21–C5	1.083	1.084	∠H21–C5–C7	118.05	116.59	H21–C5–C7–C9	−16.97	0.0
H23–C7	1.083	1.074	∠H23–C7–C5	116.56	121.06	H23–C7–C5–C3	2.43	0.0
			∠H23–C7–C9	116.62	120.78	H23–C7–C9–C11	0.94	0.0
H25–C9	1.084	1.083	∠H25–C9–C7	117.34	116.93	H25–C9–C7–C5	10.79	0.0
H27–C11	1.079	1.075	∠H27–C11–C9	117.82	119.53	H27–C11–C9–C7	1.55	−0.08
H29–C13	1.078	1.075	∠H29–C13–C11	116.90	117.50	H29–C13–C11–C9	1.46	0.12
H31–C15	1.075	1.074	∠H31–C15–C13	121.38	121.49	H31–C15–C13–C11	−0.34	−0.03
H33–C15	1.073	1.071	∠H33–C15–C13	121.51	121.12	H33–C15–C13–C11	−179.33	179.96

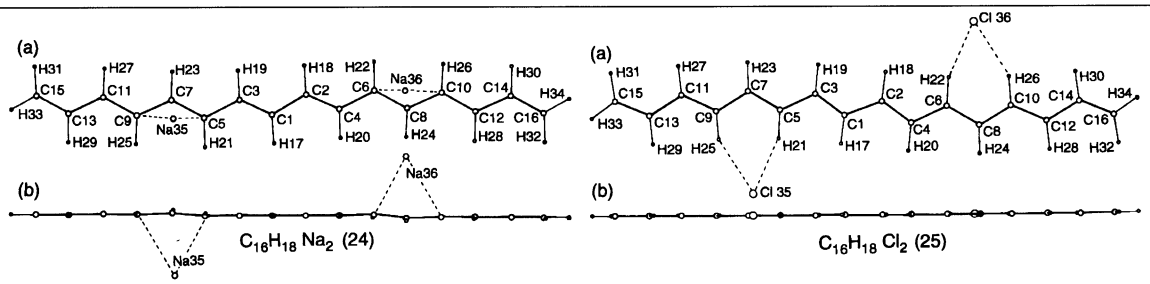

polyacetylene can contain many open-shell–**O**–units which are connected by the **A**–**E**–**A** groups. If the **O** group is not sandwiched by the **A** groups, but is connected directly to the **E** chain, the combined chain becomes an odd polyene radical chain, which is chemically and physically unstable.

Unpaired electrons of the open-shell unit contribute to metallic conduction. Keeping unpaired electrons stably in the doped chain is essential for a polymer to show metallic properties. The polson structure is a fundamental unit for doped polyacetylene to have an unpaired electron and to be metallic. An energy band calculation concerning the polson chain will be discussed in a succeeding paper.

4. Class-(4) Complexes. The class-(4) complexes are dimers of class-(1) and -(2) complexes. One comprises two class-(1) complexes, and the other comprises two class-(2) complexes. The two units are joined by the end groups, **E**, with an inversion symmetry, where the center of symmetry is placed in the middle of the connecting bond. When the chain related by an inversion is indicated by ( )*, the two types of the complexes are expressed as **E**–**A**–**E**–(**E**–**A**–**E**)* and **O**–**A**–**E**–(**E**–**A**–**O**)*, respectively.

The optimized structures and the molecular orbitals of the singlet $C_6H_8Li_2$ (**22**) and $C_{14}H_{16}Na_2$ (**23**) were calculated. The geometry of **23** is shown in Table 6. As shown in the figure of Table 6, two Na ions are located at opposite sides of the polyene chain to each other. The bond lengths of the chain between the two **A** groups clearly show bond alternation. The total atomic charges are given in Fig. 7. The distributions of excess charge on $C_6H_8Li_2$ (**22**) and $C_{14}H_{16}Na_2$ (**23**) are exactly the same value as those in C_3H_5Li and C_7H_9Na

Table 8. Optimized Geometrical Parameters in the Region around the Coordination Bonding. Dopant atoms, Na, Li, and Cl, are expressed as 'Dp', carbon atoms as A,B,C,D,E,F, and G, and hydrogen atoms as H_a, H_b, and H_c. The correspondence between these symbols and the positions of atoms are illustrated in the attached figure.

Basis set	Li complexes			Na complexes				Cl complexes		
3-21G	Class(1)	Class(2)	Class(3)	Class(1)	Class(1)	Class(1)	Class(2)	Class(1)	Class(1)	Class(2)
	(8)	**(12)**	**(19)**	**(6)**	**(9)**	**(13)**	**(15)**	**(7)**	**(10)**	**(16)**
Complexes	C_7H_9Li singlet	$C_8H_{10}Li$ doublet	$C_9H_{11}Li_2$ doublet	C_5H_7Na singlet	C_7H_9Na singlet	$C_9H_{11}Na$ triplet	$C_8H_{10}Na$ doublet	C_5H_7Cl singlet	C_7H_9Cl singlet	$C_8H_{10}Cl$ doublet
Molecular symmetry	Cs	C_1	Cs	C_1	Cs	Cs	C_1	Cs	C_{2v}	Cs
Atomic distance (Å)										
Dp–A	2.107	2.087	2.117	2.438	2.442	2.441	2.398	3.851	3.831	3.810
Dp–B	2.176	2.270	2.349	2.455	2.507	2.510	2.598	3.467	3.329	3.342
Dp–C	2.176	2.163	2.065	2.529	2.507	2.510	2.518	3.218	3.329	3.321
Dp–Hb								2.516	2.308	2.337
Dp–Hc								2.154	2.308	2.307
A–B	1.393	1.402	1.389	1.395	1.391	1.396	1.403	1.350	1.377	1.386
A–C	1.393	1.411	1.431	1.389	1.391	1.396	1.411	1.404	1.377	1.385
D–B	1.456	1.418	1.428	—	1.450	1.453	1.409	—	1.432	1.399
E–C	1.456	1.441	—	1.450	1.450	1.453	1.430	1.417	1.432	1.416
F–D	1.327	1.409	1.396	—	1.330	1.390	1.413	—	1.332	1.407
G–E	1.327	1.350	—	1.330	1.330	1.390	1.359	1.339	1.332	1.358
Ha–A	1.082	1.080	1.080	1.082	1.083	1.083	1.082	1.072	1.073	1.075
Hb–B	1.084	1.085	1.085	1.082	1.083	1.084	1.085	1.081	1.084	1.083
Hc–C	1.084	1.084	1.083	1.083	1.083	1.084	1.084	1.089	1.084	1.084
Bond angle (deg.)										
∠Dp–A–B	73.71	78.48	81.27	74.13	76.25	76.37	81.69	63.54	58.65	60.09
∠Dp–A–C	73.71	73.53	68.08	77.39	76.25	76.37	78.03	53.42	58.65	59.20
∠Dp–A–Ha	118.81	115.45	116.89	117.66	116.77	116.87	110.91	174.43	180.00	179.53
∠B–A–C	126.22	125.07	125.45	128.05	127.87	128.09	126.02	116.96	117.30	119.29
∠D–B–A	122.56	125.35	125.01	—	122.70	122.62	126.01	—	125.22	123.29
∠E–C–A	122.56	123.58	—	122.80	122.70	122.62	124.41	126.37	125.22	123.77
∠F–D–B	126.73	124.25	124.61	—	127.34	125.19	124.49	—	119.33	121.40
∠G–E–C	126.73	126.31	—	127.51	127.34	125.19	126.65	117.56	119.33	120.43
∠Ha–A–B	116.49	117.26	116.79	115.90	115.91	115.82	116.93	122.03	121.35	120.39
∠Ha–A–C	116.49	117.33	117.16	115.69	115.91	115.82	117.02	121.01	121.35	120.32
∠Hb–B–A	118.26	117.37	117.73	118.98	118.38	117.93	117.12	119.88	116.87	116.98
∠Hc–C–A	118.26	117.79	117.20	118.44	118.38	117.93	117.84	116.04	116.87	116.91
Dihedral angle (deg.)										
Dp–A(Ha)–B	85.21	89.79	93.75	84.92	87.09	87.23	91.18			
Dp–A(Ha)–C	−85.21	−83.83	−77.86	−88.78	−87.09	−87.23	−86.88			
D–B–A–C	−175.55	−173.05	−173.54	—	−178.70	−180.46	−174.10			
E–C–A–B	175.55	176.71	—	177.72	178.70	180.46	177.94			
F–D–B–A	−170.66	−176.24	−175.24	—	−171.57	−169.95	−178.43			
G–E–C–A	170.66	171.71	—	173.21	171.57	169.95	176.02			
Ha–A–B–D	−6.19	0.03	−2.71	—	−5.35	−6.81	3.77			
Ha–A–C–E	6.19	3.63	—	4.93	5.35	6.81	0.07			
Hb–B–A–C	22.77	15.32	15.08	23.28	17.58	18.14	10.29			
Hc–C–A–B	−22.77	−20.24	−33.18	−17.15	−17.58	−18.14	−12.75			

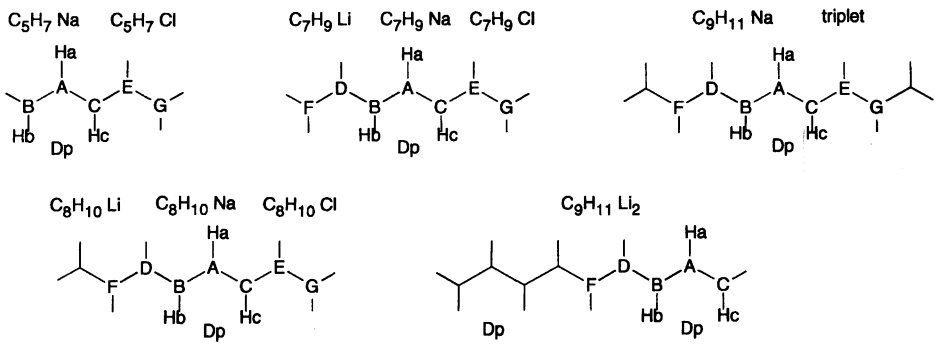

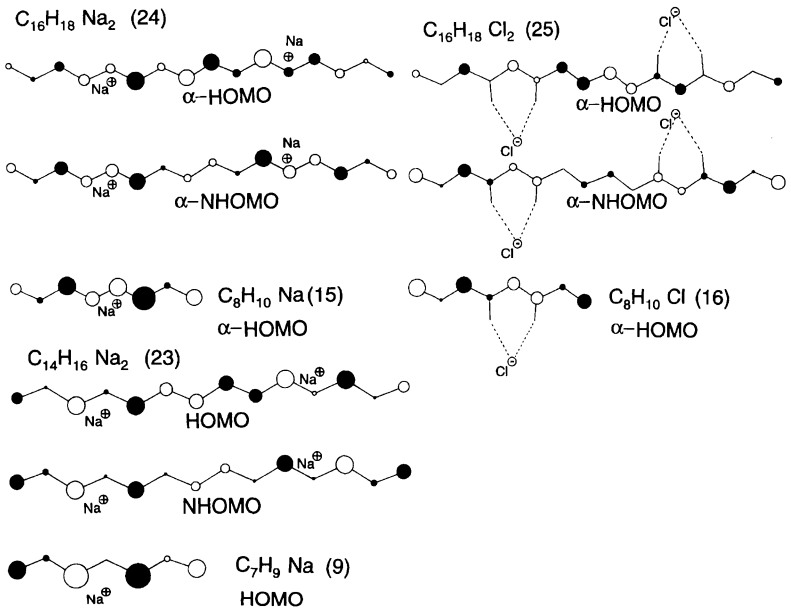

Fig. 10. MO coefficients of class-(4) complexes; $C_{14}H_{16}Na_2$ (**23**), $C_{16}H_{18}Na_2$ (triplet) (**24**), and $C_{16}H_{18}Cl_2$(triplet) (**25**).

of the class-(1) complex, respectively. The patterns of the HOMO and NHOMO of $C_{14}H_{16}Na_2$ (**23**) (Fig. 10) are antisymmetric and symmetric combinations of the HOMO of C_7H_9Na (**9**).

Next, the dimer of a class-(2) complex is discussed. The optimized structures and molecular orbitals of triplet complexes, $C_{16}H_{18}Na_2$ (**24**) and $C_{16}H_{18}Cl_2$(**25**), were calculated; the geometries are shown in Table 7. The complexes have effective spin densities in the two allyl groups at both ends (Figs. 7 and 10). The excess charge exists mostly in the **A** region, as is found in class-(1), -(2), and -(3) complexes. Accordingly, the chain structure is represented by **O**–**A**–**E**–(**E**–**A**–**O**)*, where the unpaired electrons are on the **O** groups. The chain of central **E**–**E***, C3–C1–C2–C4, clearly shows bond alternation.

The MO coefficients of the triplet $C_{16}H_{18}Na_2$ (**24**) and $C_{16}H_{18}Cl_2$(**25**) are illustrated in Fig. 10. The patterns of the α-HOMO and α-NHOMO are obtained by antisymmetric and symmetric combinations of the HOMO of $C_8H_{10}Na$ (**15**) and $C_8H_{10}Cl$ (**16**), respectively.

In both types of complexes discussed in this section, the central carbon chain connecting the **A** groups is a normal conjugated double bond, **E**. This indicates that the **A** group shields the central carbon chain from the influence of the **O** group and vice versa. The central **A**–**E**–(**E**–**A**)* chain of the triplet complex connects the two **O** units, thus, keeping an unpaired electron on each end groups. If two polson units (class-(3) complex) are connected, a polson–antipolson pair, **E**–**A**–**O**–**A**–**E**–(**E**–**A**–**O**–**A**–**E**)* is obtained. Since **O**–**A**–**E**–(**E**–**A**–**O**)* is the central part of the polson–antipolson pair, the structure of triplet complexes **24** and **25** show a geometry which connects the two polson units.

Although the doping process of **24**, (n-doping), is different from that of **25**, (p-doping), the both complexes have a common feature in the patterns of MO coefficients in the region of **O** groups. Both complexes have **O** groups at both ends of the chain. Each **O** group has an unpaired electron. The interaction between the α-HOMO's of **O** groups produces the α-HOMO and α-NHOMO of the complex. The pattern of the MO coefficients show that the α-HOMO and α-NHOMO are antisymmetric and symmetric combinations of the α-HOMO's of **O** groups, respectively. This represents a basic interaction to form a one-dimensional metallic energy band. The chain structures of **24** and **25** are used in an energy band calculation in the succeeding paper. Chain structures with many polson units have a conduction band which is half filled with electrons. This is the actual case expected in metallic doped polyacetylene.

Conclusion

This paper presents optimized structures and MO's of fundamental model compounds of doped polyacetylene. The mode of coordination of Na, Li, and Cl to *trans*-polyene chain is clarified. The polson structure, a class-(3) complex, is an essential unit for heavily doped polyacetylene to be metallic. It includes an unpaired electron and can form a metallic energy band when they are properly joined with long polyene by forming [–(polyene)–(polson)–(polyene)–(antipolson)–(polyene)–]$_n$ chain. This point will be discussed in the succeeding paper. A basic pattern of the interaction between the MO's of a singly doped chain is found in the MO's of class-(4) complexes. The symmetric combination of two MO is more stable than that of the antisymmetric combination. The change in the orbital energies of MO by forming a dimer and a polymer will be discussed in

the succeeding paper.

We are indebted to grants in aid of Ministry of Education, Culture and Science, No. 02453010 and also for International Joint Research Project from the NEDO (New Energy and Industrial Technology Development Organization), Japan. We thank the computer center of the Institute for Molecular Science, for the use of the HITAC M-680H and Gaussian programs. We are also grateful to Prof. Kimihiko Hirao of Nagoya University and Dr. Nobuaki. Koga of Institute for Molecular Science for helpful advice on calculation.

References

1) M. J. Rice, *Phys. Lett.*, **71A**, 152 (1979).
2) W. P. Su, J. R. Schrieffer, and A. J. Heegr, *Phys. Rev. Lett.*, **42**, 1698 (1979).
3) S. Kivelson and A. J. Heeger, *Phys. Rev. Lett.*, **55**, 308 (1985).
4) C. Tanaka and J. Tanaka, *Mat. Res. Soc. Symp. Proc.*, **247**, 577 (1992).
5) A. J. Heeger, S. Kivelson, J. R. Schrieffer, and W. P. Su, *Rev. Mod. Phys.*, **60**, 781 (1988).
6) A. J. Heeger, *Faraday Discuss. Chem. Soc.*, **88**, 203 (1989).
7) C. Tanaka and J. Tanaka, *Synth. Metals*, **43**, 3709 (1991).
8) J. Tanaka and C. Tanaka, "Proceedings of the Eighty-first Nobel Symposium, Conjugated Polymers and Related Materials: The Interconnection of Chemical and Electronic Structure," ed by W. R. Salaneck, I. Lunström, and B. Rånby, Oxford University Press, Oxford (1993), p. 239.
9) J. Tanaka, Y. Saito, M. shimizu, C. Tanaka, and M. Tanaka, *Bull. Chem. Soc. Jpn.*, **60**, 1595 (1987).
10) J. S. Binkley, M. J. Frisch, D. J. Defrees, K. Raghavachari, R. A. Whiteside, H. B. Schlegel, and J. A. Pople, "Gaussian 82," Carnegie-Mellon Chemistry Publishing Unit, Pittsburgh, PA 15213 U.S.A. (1984), registered as IMS program by N. Koga.
11) M. J. Frisch et al., "Gaussian 86," Carnegie-Mellon Quantum Chemistry Publishing Unit, Pittsburgh, PA 15213 U.S.A. (1986). IMS adaptation is written by N. Koga et al. Institute for Molecular Science, Okazaki 444, Japan.
12) S. K. Arora, R. B. Bates, W. A. Beavers, and R. S. Cutler, *J. Am. Chem. Soc.*, **97**, 6271 (1975).
13) E. Hirota, C. Yamada, and M. Okunishi, *J. Chem. Phys.*, **97**, 2963 (1992).
14) K. Nukasawa, J. Tanaka, and S. Nagakura, *J. Phys. Soc. Jpn.*, **8**, 792 (1953).
15) J. N. Murrell, S. F. A. Kettle, and J. M. Tedder, "Valence Theory," John Wiley, London (1969), p. 278.